A Constitutive Model for Plastics with Piecewise Linear Yield Surface and Damage

M. Vogler[1], S. Kolling[2], A. Haufe[3]

[1] Leibniz University Hannover, Institute for Structural Analysis, 30167 Hannover
[2] DaimlerChrysler AG, EP/SPB, HPC X271, 71059 Sindelfingen
[3] Dynamore GmbH, Industriestr. 2, D-70565 Stuttgart, Germany

Abstract:

Reliable prediction of the behaviour of structures made from polymers is a topic under considerable investigation in engineering practice. Especially, if the structure is subjected to dynamic loading, constitutive models considering the mechanical behaviour properly are not available in commercial finite element codes yet. A constitutive model is derived including important phenomena like necking, crazing, strain rate dependency, unloading behaviour and damage. In particular, different yield surfaces in compression and tension and strain rate dependent failure, the latter with damage induced erosion, are taken into account. With the present formulation, standard verification tests can be simulated successfully. Also, an elastic damage model can be used to approximate the unloading behaviour of thermoplastics adequately.

Keywords:

Non-Isochoric Plasticity, Visco-Plasticity, Damage, Failure

1 Introduction

In engineering practice, the commonly used model for thermoplastics is a visco-plastic approach based on von Mises plasticity [2]. However, most thermoplastics exhibit a different behaviour in tension, compression and shear, so the assumption of a von Mises yield locus is not justifiable. Furthermore crazing, a localized deformation process which goes along with a permanent increase of volume and a low biaxial strength, can't be modelled so far. To simulate crazing it may therefore be desirable to consider biaxial test data in the numerical model. In the last few years, a lot of theoretical work has been performed to find an appropriate yield surface for the description of thermoplastics, see [18], [11], [24] and [25] among others. In the present material model termed PLYS (PIECEWISE LINEAR YIELD SURFACE), we provide a pressure dependent multi-surface $\mathcal{C}^0$-differentiable yield locus, which consists of up to four Drucker-Prager cones, depending on the available experimental data. To generate this yield locus test data from uniaxial tension and compression tests, from a shear test and from biaxial tension and (if available) compression tests can be regarded. Another drawback is the assumption of plastic incompressibility which is clearly not correct for thermoplastics. Here a plastic potential with a quadratic dependency in pressure is used to account for different volumetric plastic straining under compression and tension. Strain rate dependency for the yield surface as well as for the failure onset is another key property. Furthermore, a simple but effective damage formulation that allows smooth fading of elements, that are supposed to fail, is included. The present material model PLYS is implemented as a user subroutine in the explicit solver LS-DYNA. However, the results are transferable to other solvers.

2 Constitutive model

Within PLYS additive decomposition of strain $\Delta\boldsymbol{\varepsilon} = \Delta\boldsymbol{\varepsilon}^{\mathrm{el}} + \Delta\bar{\varepsilon}^{pl}$ is assumed. This leads to an elastic stress increment $\Delta\boldsymbol{\sigma} = \mathbb{C} : \Delta\boldsymbol{\varepsilon}^{\mathrm{el}}$ where the elastic constitutive tensor reads $\mathbb{C} = 2G\boldsymbol{\delta}\otimes\boldsymbol{\delta} - (K - \frac{2}{3}G)\mathbb{I}$. Here G is the shear and K the bulk modulus, $\boldsymbol{\delta}$ and $\mathbb{I}$ represent the second and fourth order unit tensor, respectively. The plastic strain components are calculated by a classical elastic predictor plastic corrector scheme.

2.1 Definition of the yield surface

The yield surface is divided into up to four Drucker-Prager-cones, depending on the available experimental data:

$$f(p, q, \bar{\varepsilon}^{pl}, \dot{\bar{\varepsilon}}^{pl}) = q - \beta(\bar{\varepsilon}^{pl}, \dot{\bar{\varepsilon}}^{pl})p - c(\bar{\varepsilon}^{pl}\dot{\bar{\varepsilon}}^{pl}) \tag{1}$$

with

$$\begin{array}{ll}
\beta(\bar{\varepsilon}^{pl}) = 3\frac{\sigma_y^t(\bar{\varepsilon}^{pl})-\sigma_y^{bt}(\bar{\varepsilon}^{pl})}{2\sigma^{bt}(\bar{\varepsilon}^{pl})-\sigma_y^t(\bar{\varepsilon}^{pl})} & c(\bar{\varepsilon}^{pl}\dot{\bar{\varepsilon}}^{pl}) = \xi(\dot{\bar{\varepsilon}}^{pl})[\sigma_y^t(\bar{\varepsilon}^{pl}) + \beta(\bar{\varepsilon}^{pl})\frac{\sigma_y^t(\bar{\varepsilon}^{pl})}{3}] \quad \text{for} \quad p < -\frac{q}{3} \\
\beta(\bar{\varepsilon}^{pl}) = -3\frac{\sigma_y^s(\bar{\varepsilon}^{pl})-\sigma_y^t(\bar{\varepsilon}^{pl})}{\sigma_y^t(\bar{\varepsilon}^{pl}}) & c(\bar{\varepsilon}^{pl}\dot{\bar{\varepsilon}}^{pl}) = \xi(\dot{\bar{\varepsilon}}^{pl})\sigma_y^s(\bar{\varepsilon}^{pl}) \quad \text{for} \quad -\frac{q}{3} \le p < 0 \\
\beta(\bar{\varepsilon}^{pl}) = 3\frac{\sigma_y^c(\bar{\varepsilon}^{pl})-\sigma_y^s(\bar{\varepsilon}^{pl})}{\sigma_y^c(\bar{\varepsilon}^{pl})} & c(\bar{\varepsilon}^{pl}\dot{\bar{\varepsilon}}^{pl}) = \xi(\dot{\bar{\varepsilon}}^{pl})\sigma_y^s(\bar{\varepsilon}^{pl}) \quad \text{for} \quad 0 \le p < \frac{q}{3} \\
\beta(\bar{\varepsilon}^{pl}) = 3\frac{\sigma_y^{bc}(\bar{\varepsilon}^{pl})-\sigma_y^c(\bar{\varepsilon}^{pl})}{2\sigma_y^{bc}(\bar{\varepsilon}^{pl})-\sigma_y^c(\bar{\varepsilon}^{pl})} & c(\bar{\varepsilon}^{pl}\dot{\bar{\varepsilon}}^{pl}) = \xi(\dot{\bar{\varepsilon}}^{pl})[\sigma_y^c(\bar{\varepsilon}^{pl}) - \beta(\bar{\varepsilon}^{pl})\frac{\sigma_y^c(\bar{\varepsilon}^{pl})}{3}] \quad \text{for} \quad \frac{q}{3} \le p
\end{array} \tag{2}$$

Here $p = -\frac{1}{3}\text{tr}\boldsymbol{\sigma} = -\frac{1}{3}I_1$ represents the hydrostatic axis (I_1 is the first invariant of the stress tensor $\boldsymbol{\sigma}$) and $q = \sqrt{\frac{3}{2}\boldsymbol{s} : \boldsymbol{s}} = 3J_2$ the deviatoric axis (J_2 is the second invariant of the stress deviator $\boldsymbol{s} = \boldsymbol{\sigma} - \frac{1}{3}\text{tr}\boldsymbol{\sigma}\boldsymbol{\delta}$). The parameter $\beta(\bar{\varepsilon}^{pl})$ is calculated from the hardening curves $\sigma_y^t(\bar{\varepsilon}^{pl}\dot{\bar{\varepsilon}}^{pl})$, $\sigma_y^c(\bar{\varepsilon}^{pl})$, $\sigma_y^s(\bar{\varepsilon}^{pl})$, $\sigma_y^{bt}(\bar{\varepsilon}^{pl})$ and $\sigma_y^{bc}(\bar{\varepsilon}^{pl})$ which can be obtained directly from uniaxial tension and compression tests, from shear tests and from biaxial tension and (if available) compression tests. The factor $\xi(\dot{\bar{\varepsilon}}^{pl})$ is obtained from dynamic uniaxial tensile test and regards the strain rate dependency of the material (see section "Rate effects"). The yield surface is illustrated in Figure 4. Although experimental data of up to 5 material tests can be regarded to assemble the piecewise linear yield surface, the most important and the most reliable material test is still the uniaxial tensile test. There a nearly pure uniaxial stress state can be assumed during the whole test. To account for the effect, that most polymers behave stiffer under compression than under tension, test data from compression tests are needed. These tests are more complicated than uniaxial tensile tests and a certain interaction with tension and shear cannot be avoided completely. This applies also for biaxial compression tests and so these test data, even if they are available, should be used with care. But in fact a pure biaxial stress state is not only hard to achieve in an experiment, but also in simulating structural parts and so these test data are of minor importance and can first be neglected. To account for the effect of crazing, it is desirable to include test data from biaxial tensile tests. Crazing accompanies with a permanent increase of volume (volumetric plastic straining) and a low biaxial strength. Some polymeric materials exhibit a different behaviour also under pure shear stress states. Therefore also test data from pure shear tests can be regarded.

2.2 Hardening formulation

In the present material model PIECEWISE LINEAR YIELD SURFACE (PLYS) the hardening formulation is fully tabulated and consequently the user can directly input measurement results from uniaxial tension, uniaxial compression, shear tests, biaxial tension and (if available) biaxial compression tests. In the material model load curves giving the yield stress as a function of the corresponding plastic strain are needed, but in experiments mostly the yield stress over the total strain is measured. So, assuming an additive decomposition of the strain increments $\Delta\boldsymbol{\varepsilon} = \Delta\boldsymbol{\varepsilon}^{\text{el}} + \Delta\bar{\varepsilon}^{pl}$, the experimentally obtained hardening curves must be modified by just subtracting the elastic strain component from the total strain increment as shown in Figure 1. So all available test data can be feed directly into the material model. No fitting of coefficients is required. The test results,

that are reflected in the load curves, will be used exactly by PLYS without fitting to any analytical expression. Thus, there is no need of time consuming parameter identification. In the material card for PLYS LOADCURVE-ID's for up to 5 hardening curves (uniaxial tension and compression, biaxial tension and compression and shear tests) can be assigned, but the programm recognizes the available LOADCURVES. If there are not all of the test data available the program recognizes the missing experimental data automatically and the piecewise linear yield surface is assembled from the provided test data. That means if there are LCID's only assigned for test data from uniaxial compression tests and uniaxial tensile tests a simple DRUCKER-PRAGER material model is realized and if only test data from uniaxial tensile tests are provided, the von Mises yield locus is recovered. This procedure allows a straight forward treatment in engineering practise. The load curves that are expected as input are briefly described here:

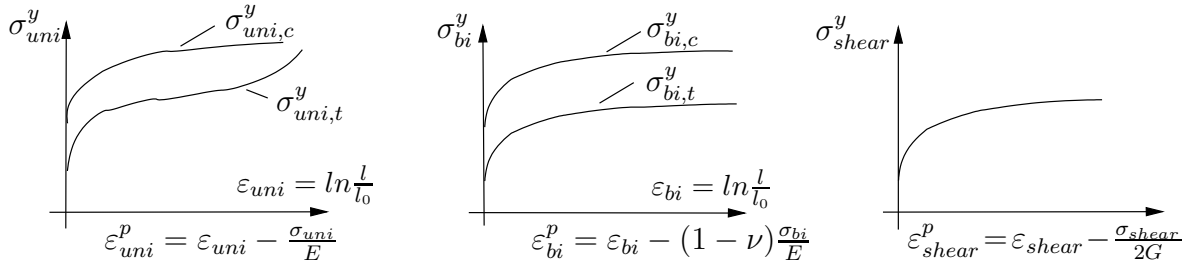

Figure 1: Uniaxial, biaxial and shear hardening curves from experiments

Up to five table lookups will be performed in each iteration during each time step. As input data serves the plastic strain for uniaxial and biaxial tension and compression and for shear. The table lookup delivers the current yield value as well as the tangent with respect to the plastic strain:

$$\varepsilon^p_{uni,t} \Rightarrow \sigma^y_{uni,t},\ \frac{\partial\sigma^y_{uni,t}}{\partial\varepsilon^p_{uni,t}}, \quad \varepsilon^p_{uni,c} \Rightarrow \sigma^y_{uni,c},\ \frac{\partial\sigma^y_{uni,c}}{\partial\varepsilon^p_{uni,c}},$$

$$\varepsilon^p_{bi,t} \Rightarrow \sigma^y_{bi,t},\ \frac{\partial\sigma^y_{bi,t}}{\partial\varepsilon^p_{bi,t}}, \quad \varepsilon^p_{bi,c} \Rightarrow \sigma^y_{bi,c},\ \frac{\partial\sigma^y_{bi,c}}{\partial\varepsilon^p_{bi,c}}, \quad \varepsilon^p_{shear} \Rightarrow \sigma^y_{shear},\ \frac{\partial\sigma^y_{shear}}{\partial\varepsilon^p_{shear}}.$$

Care must be taken to ascertain the von Mises stress σ_{vm} and the equivalent plastic strain $\bar{\varepsilon}^{pl}$ from the experimentally obtained data. This is done in the material routine. Table 1 shows the relations between the stresses and strains obtained from experiment and the von Mises stress σ_{vm} or q and the equivalent plastic strain.

2.3 Rate effects

Plastics are usually highly rate dependent. A proper visco-plastic consideration of the rate effects is therefore important to the numerical treatment of the material law. Rate effects can only be derived sufficiently from uniaxial tensile tests, therefore data to determine the rate dependency are based on uniaxial dynamic testing. Simplifying, it is assumed, that the strain rate sensitivity in all stress states is the same as in tension. Otherwise

experiment	hydro-static pressure p	v.Mises stress $q = \sigma_{vm}$	equivalent plastic strain $\bar{\varepsilon}^{pl}$	volumetric plastic strain ε_v^{pl}
uniaxial tension	$-\frac{1}{3}\sigma_t$	σ_t	$\frac{2}{3}(1+\nu_p)\varepsilon_t^p$	$(1-2\nu_p)\varepsilon_t^p$
uniaxial compression	$\frac{1}{3}\sigma_c$	σ_c	$\frac{2}{3}(1+\nu_p)\varepsilon_c^p$	$-(1-2\nu_p)\varepsilon_c^p$
biaxial tension	$-\frac{2}{3}\sigma_{bt}$	σ_{bt}	$\frac{2}{3}\frac{1+\nu_p}{1-\nu_p}\varepsilon_{bt}^p$	$2\frac{1-2\nu_p}{1-\nu_p}\varepsilon_{bt}^p$
biaxial compression	$\frac{2}{3}\sigma_{bc}$	σ_{bc}	$\frac{2}{3}\frac{1+\nu_p}{1-\nu_p}\varepsilon_{bc}^p$	$-2\frac{1-2\nu_p}{1-\nu_p}\varepsilon_{bc}^p$
pure shear	0	$\sqrt{3}\sigma_s$	$\frac{2}{\sqrt{3}}\lvert\varepsilon_s^p\rvert$	0

Table 1: Relations between experimental data and computational values

tests at different strain rates for all other material tests have to be performed. The strain rate dependency obtained from tensile tests is transferred via a factor $\xi(\dot{\bar{\varepsilon}}^{pl})$ to the other quasi-static hardening curves:

$$\xi(\dot{\bar{\varepsilon}}^{pl}) = \frac{\sigma(\bar{\varepsilon}^{pl}, \dot{\bar{\varepsilon}}^{pl})}{\sigma(\bar{\varepsilon}^{pl}, \dot{\bar{\varepsilon}}^{pl} = 0)} \tag{3}$$

If dynamic tests are available , the load curve defining the yield stress in uniaxial tension is simply replaced by a table definition. Similar to MAT 24 in LS-DYNA this table contains multiple load curves corresponding to different values of the plastic strain rate as illustrated in Figure 2. Input data for the table lookup are the current uniaxial plastic

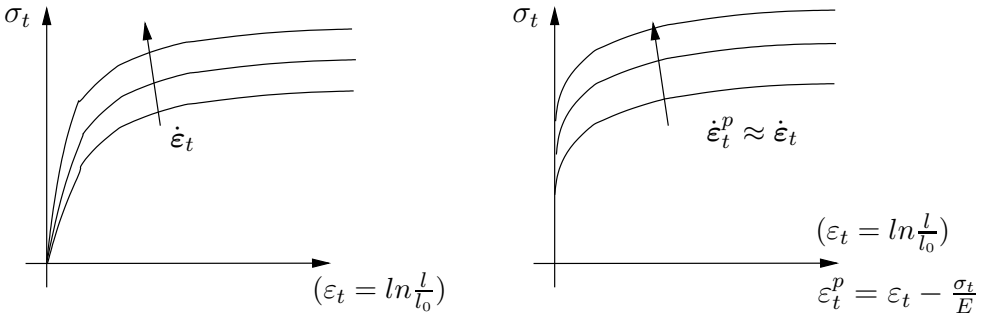

Figure 2: Tensile hardening curve from dynamic tensile test

strain and the current uniaxial plastic strain rate, the table lookup delivers the yield value in uniaxial tension and the tangents with respect of the plastic strain and the plastic strain rate:

$$\varepsilon_{uni,t}^p,\ \dot{\varepsilon}_{uni,t}^p,\ \Rightarrow\ \sigma_{uni,t}^y,\ \frac{\partial\sigma_{uni,t}^y}{\partial\varepsilon_{uni,t}^p},\ \frac{\partial\sigma_{uni,t}^y}{\partial\dot{\varepsilon}_{uni,t}^p} \tag{4}$$

2.4 Plastic potential

In the present material model, PLYS, a non-associated flow rule is assumed. The plastic potential gives the direction $\mathbf{m}$ for the plastic flow. So the plastic strain rate is given as:

$$\dot{\varepsilon}_p = \dot{\lambda}\,\|\mathbf{m}\| = \dot{\lambda}\left\|\frac{\partial g}{\partial \boldsymbol{\sigma}}\right\|, \quad \left\|\frac{\partial g}{\partial \boldsymbol{\sigma}}\right\| = \sqrt{\frac{\partial g}{\partial \boldsymbol{\sigma}} : \frac{\partial g}{\partial \boldsymbol{\sigma}}} \tag{5}$$

whereas $\boldsymbol{m}$ is the direction of the plastic flow given by the plastic potential g and $\dot{\lambda}$ is the rate of the plastic multiplier. The volumetric plastic strain rate, the deviatoric plastic strain rate and the equivalent plastic strain rate are defined as:

$$\dot{\varepsilon}_{pv} = tr(\dot{\boldsymbol{\varepsilon}}_p) = \frac{\dot{\lambda}}{\| \frac{\partial g}{\partial \boldsymbol{\sigma}} \|} tr\Big(\frac{\partial g}{\partial \boldsymbol{\sigma}}\Big) \tag{6}$$

$$\dot{\boldsymbol{\varepsilon}}_{pd} = \dot{\boldsymbol{\varepsilon}}_p - \frac{\dot{\boldsymbol{\varepsilon}}_{vp}}{3}\boldsymbol{\delta} \tag{7}$$

$$\dot{\bar{\varepsilon}}_p = \sqrt{\frac{2}{3}\dot{\boldsymbol{\varepsilon}}_{pd}{:}\dot{\boldsymbol{\varepsilon}}_{pd}} = \frac{\dot{\lambda}}{\| \frac{\partial g}{\partial \boldsymbol{\sigma}} \|}\sqrt{\frac{2}{3}\frac{\partial g}{\partial \boldsymbol{\sigma}}\Big|_d : \frac{\partial g}{\partial \boldsymbol{\sigma}}\Big|_d} \tag{8}$$

The plastic potential g is defined as:

$$g = \sqrt{q^2 + \alpha p^2} \tag{9}$$

The amount of dilatancy or compression, i.e. the increase or decrease in material volume due to yielding, can be controlled with the flow parameter α, whereas α correlates to the plastic poisson ratio:

$$\nu_p = \frac{9 - 2\alpha}{18 + 2\alpha} \Rightarrow \alpha = \frac{9}{2}\left(\frac{1 - 2\nu_p}{1 + \nu_p}\right) \tag{10}$$

Plausible flow behaviour means that $0 \le \alpha \le \frac{9}{2} \Rightarrow 0 \le \nu_p \le 0.5$. If the flow parameter α is set to zero, there is no change in material volume when yielding occurs and the von Mises flow potential is recovered. It is emphasized that the flow parameter α, respective ν_p is not a material constant. The flow parameter changes with progressing plastic straining. For a wide range of thermoplastics the Poisson ratio at the beginning of plastic deformation is between 0.4 and 0.5 and with further plastic deformation ν_p decreases and, especially when crazing occurs, ν_p reduces to zero. So there is a nearly foam-like behaviour when crazing occurs. To account for the experimentally observed effect of a non-constant plastic Poisson ratio, in PLYS the value of the plastic Poisson ratio can be input either as a constant or as a load curve in function of the uniaxial plastic strain. The rate of the plastic strain tensor, the rate of the deviatoric plastic strain tensor and the volumetric plastic strain rate for the assumed plastic potential g are given as:

$$\dot{\boldsymbol{\varepsilon}}^p = \frac{\dot{\lambda}}{g}\left(\frac{3}{2}\boldsymbol{s} + \frac{1}{3}\alpha p\boldsymbol{\delta}\right) \tag{11}$$

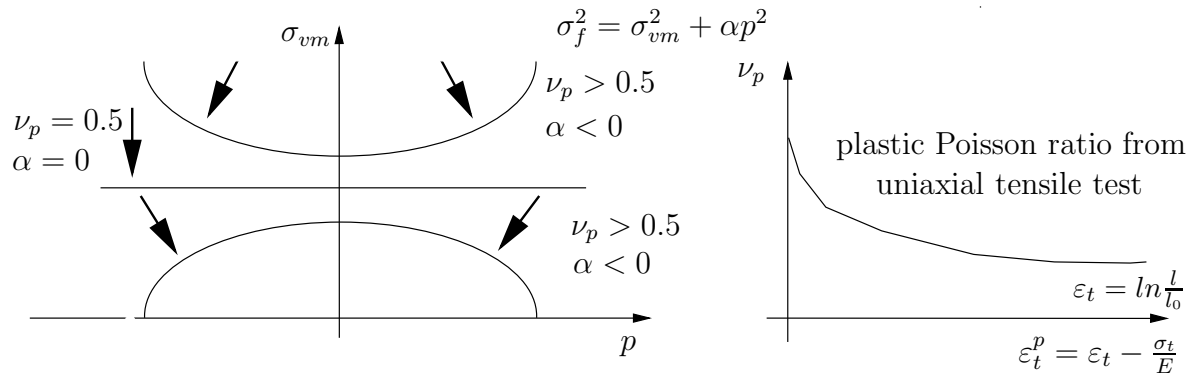

Figure 3: Influence of the flow rule on the plastic Poisson ratio

Here $\boldsymbol{s}$ is the stress deviator and $\boldsymbol{\delta}$ is the second order unit tensor. The deviatoric plastic strain rate is given as:

$$\dot{\boldsymbol{\varepsilon}}_{dev}^p = \frac{\dot{\lambda}}{g}\frac{3}{2}\boldsymbol{s} \tag{12}$$

and the volumetric plastic strain rate is:

$$\dot{\boldsymbol{\varepsilon}}_{vol}^p = \frac{\dot{\lambda}\alpha p}{g} \tag{13}$$

The principle of the material model PLYS is summarized in Figure 4.

2.5 Damage

Numerous damage models can be found in the literature. Probably the simplest concept is elastic damage where a scalar damage parameter (usually written as d) is a function of the elastic energy and effectively reduces the elastic modulae of the material. In the case of ductile damage, d is a function of plastic straining and affects the yield stress rather than the elastic modulae. This is equivalent to plastic softening. In more sophisticated damage models, d depends on both the plastic straining and the elastic energy (and maybe other factors) and affects yield stress as well as elastic modulae. (see [9]). In the present material model PLYS a simple damage model is implemented where the damage parameter d is a function of plastic strain only. A load curve must be provided by the user giving d as a function of the true plastic strain under uniaxial tension. The value of the critical damage d_{crit} leading to rupture is then the only other required additional input. The implemented damage model is isotropic. Furthermore the model uses the notion of the effective cross section, which is the true cross section of the material minus the cracks that have developed. The effective stress as the force divided by the effective cross section is defined as

$$\sigma = \frac{F}{A},\ \sigma_{eff} = \frac{F}{A_{eff}} = \frac{F}{A(1-d)} = \frac{\sigma}{(1-d)}\,, \tag{14}$$

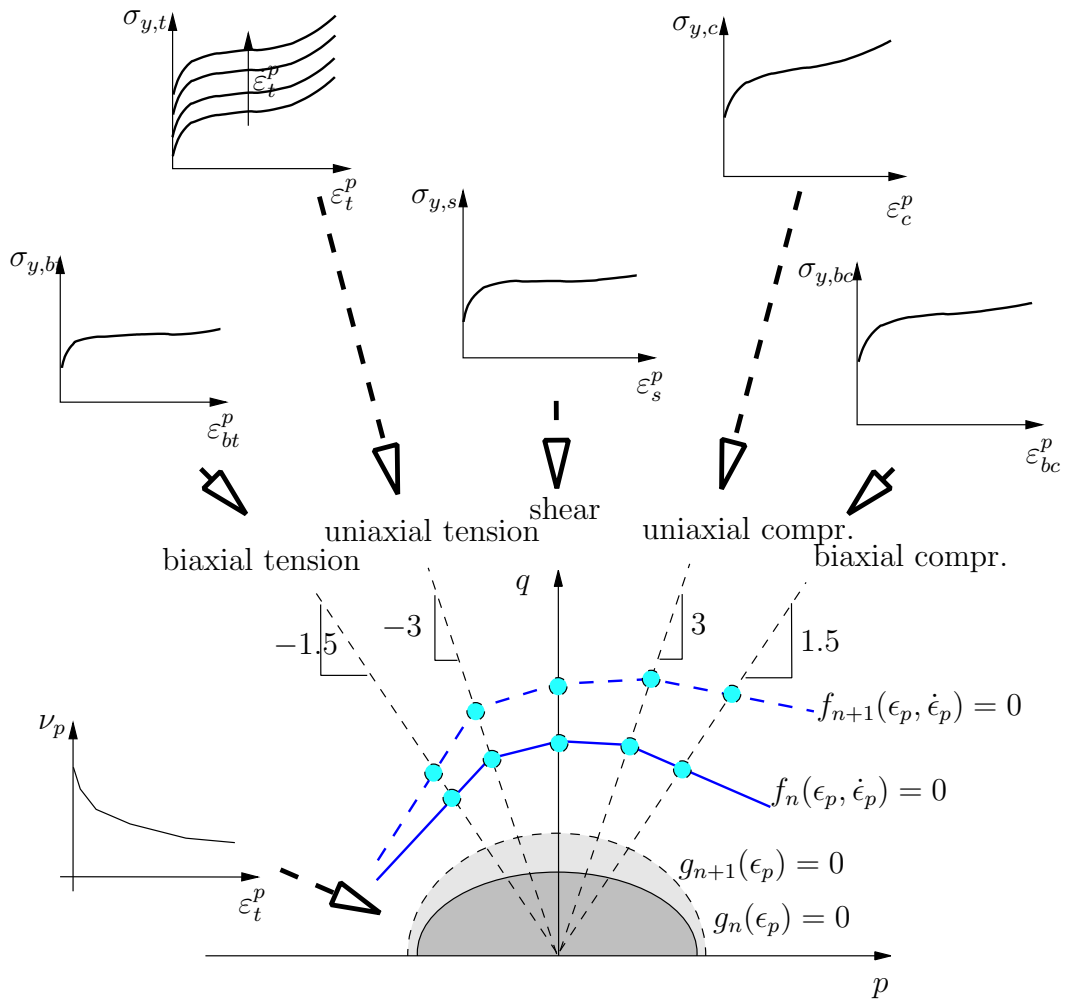

Figure 4: Scheme of PIECEWISE LINEAR YIELDSURFACE

which allows to define an effective yield stress of

$$\sigma_{y,eff} = \frac{\sigma_y}{(1-d)}\,, \tag{15}$$

see[9]. By application of the principle of strain equivalence, stating that if the undamaged modulus is used, the effective stress corresponds to the same elastic strain as the true stress using the damaged modulus, one can write:

$$E = \frac{\sigma_{eff}}{\varepsilon_e},\ E_d = \frac{\sigma}{\varepsilon_e} = E(1-d) \tag{16}$$

Note that the plastic strains are therefore the same:

$$\varepsilon_p = \varepsilon - \frac{\sigma_{eff}}{E} = \varepsilon - \frac{\sigma}{E_d} \tag{17}$$

No damage will occur under pure elastic deformation with this model. The case of a material that is perfectly plastic in its undamaged state is illustrated in Figure 5. It can

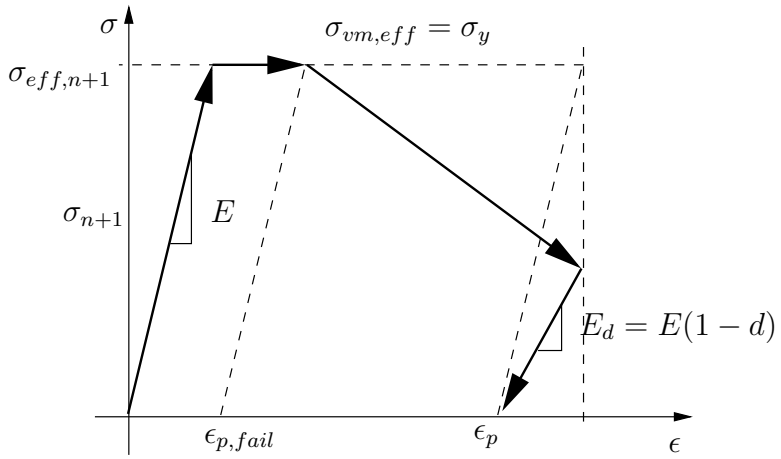

Figure 5: Damage formulation

be seen that the damage parameter effectively reduces the elastic modulus. Consequently if unloading is performed at different strain values during the uniaxial tensile test, the different unloading slopes allow to estimate the damage parameter for a given plastic strain:

$$d(\varepsilon_{pt}) = 1 - \frac{E_d(\varepsilon_{pt})}{E} \tag{18}$$

The damage model will thus be used essentially to fit the unloading behaviour of the material. The two stage process of determining input data from a measured true stress/strain curve is illustrated below. In a first step the damage curve is derived as given in Figure 6.

In a second step the hardening curve is determined in terms of effective stresses (see

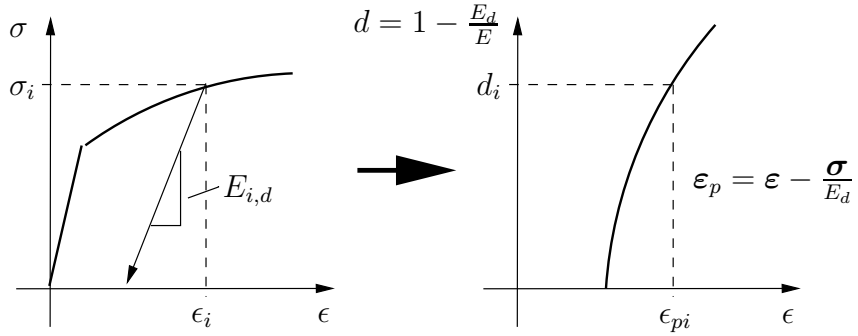

Figure 6: Determination of damage as a function of plastic strain

Figure 7). As usual the failure strain corresponds to the point where $d = 0$ and the rupture strain corresponds to the point where d reaches the critical value d_{crit}. If the damage curve is given a negative identification number in the LS-DYNA input, then the hardening curve data are expected in terms of true stresses and the input preparation

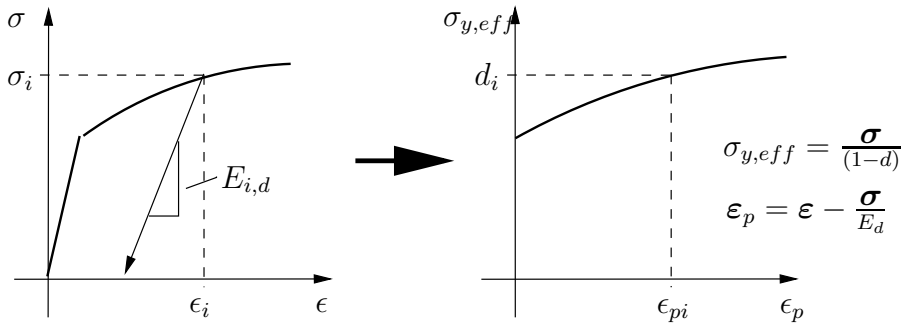

Figure 7: Conversion from true stress to effective hardening curve

is performed as if there were no damage. In this case the numerically computed stress values will correspond to the input data and the damage model will seem to affect only the elastic modulae and thus the unloading and reloading behaviour of the material.

2.6 Failure

Failure is approximated by deletion of elements dependent on strain rate $\dot{\bar{\varepsilon}}^{pl}$ and pressure p. Again, tabulated data of two curves is used to define $\bar{\varepsilon}^{pl}_{\text{fail}} = \bar{\varepsilon}^{pl}_{\text{fail,rate}}(\dot{\bar{\varepsilon}}^{pl})\xi_{\text{fail,pres}}(p)$ which determines the onset of element deletion. However, the actual deletion of the element is postponed by the user defined rupture strain $\bar{\varepsilon}^{pl}_{\text{rupt}}$. In this case the stress is scaled to $\boldsymbol{\sigma}_{\text{fail}} = \boldsymbol{\sigma}\,(1 - \zeta_{\text{fade}})$ where $\zeta_{\text{fade}} = \left\langle (\bar{\varepsilon}^{pl} - \bar{\varepsilon}^{pl}_{\text{fail}})/\bar{\varepsilon}^{pl}_{\text{rupt}} \right\rangle$ in McCauley notation. The element is finally deleted if $\zeta_{\text{fade}} \geq 0.98$ holds true. Thus, the effect of fading the failed element smoothly is achieved.

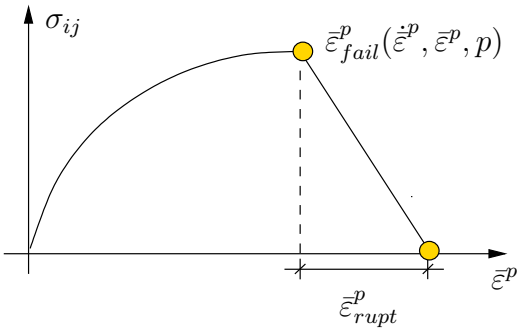

2.7 Plane stress iteration

To apply a three dimensional material model in shell elements, a plane stress iteration is required. In the material model PLYS a secant iteration is implemented. Therefore two start values $\Delta\varepsilon^1_{zz}$ and $\Delta\varepsilon^2_{zz}$ for the strain increments in thickness direction are needed. The strain component in zz-direction (thickness direction) is updated in every iteration step, until the stress component in zz-direction vanishes. To assure convergence, the solution $\sigma_{zz} = 0$ must lie in the interval $[\Delta\varepsilon^1_{zz}, \Delta\varepsilon^2_{zz}]$. That means the condition $\sigma_{zz}(\Delta\epsilon^1_{zz})\sigma_{zz}(\Delta\epsilon^2_{zz}) < 0$ must be fulfilled. The procedure for the plane stress iteration is illustrated in Figure 8. As a first start value a strain increment is chosen under the assumption of a three dimensional stress state and a pure elastic step. So the conversion

of Hooke's law delivers the first start value for the secant iteration:

$$\Delta\epsilon_{zz}^{1} = -\frac{\sigma_{zz}^{1} + \lambda(\Delta\epsilon_{xx} + \Delta\epsilon_{yy})}{\lambda + 2\mu} \tag{19}$$

As a second start value a plane stress state and plastic material behaviour are assumed. So the second start value reads:

$$\Delta\epsilon_{zz}^{2} = -\frac{\nu_p}{(1-\nu_p)}(\Delta\epsilon_{xx} + \Delta\epsilon_{yy}) \tag{20}$$

Algorithm for plane stress iteration:

1. computing first start value $\Delta\epsilon_{zz}^{1}$:

$$\Delta\epsilon_{zz}^{1} = -\frac{\sigma_{zz} + (K - \frac{2}{3}G)(\Delta\epsilon_{xx} + \Delta\epsilon_{yy})}{\frac{4}{3}G + K}$$
$$\Rightarrow \text{ plasticity algorithm} \Rightarrow \sigma_{zz}^{1}$$

2. computing second start value $\Delta\epsilon_{zz}^{2}$:

$$\Delta\epsilon_{xx}^{2} = -\frac{\nu_p}{(1-\nu)}(\Delta\epsilon_{xx} + \Delta\epsilon_{yy})$$
$$\Rightarrow \text{ plasticity algorithm} \Rightarrow \sigma_{zz}^{2}$$

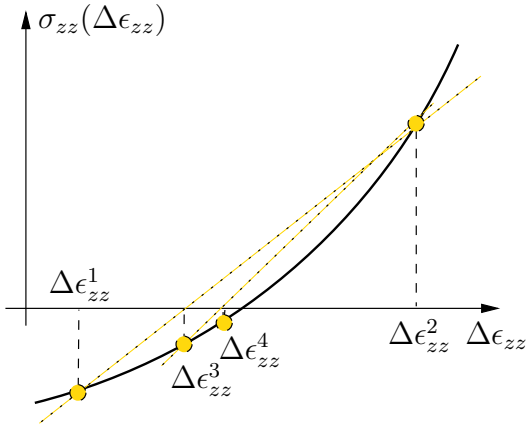

Figure 8: plane stress iteration: secant iteration

3. Secant iteration: computing strain increment $\Delta\epsilon_{zz}^{n+1}$:

$$\Delta\epsilon_{zz}^{n+1} = \Delta\epsilon_{zz}^{n-1} - \frac{\Delta\epsilon_{zz}^{n} - \Delta\epsilon_{zz}^{n-1}}{\sigma_{zz}^{n} - \sigma_{zz}^{n+1}}\sigma_{zz}^{n}$$

4. checking exit condition:

$$\text{IF} \quad \frac{|\Delta\epsilon_{zz}^{n} - \Delta\epsilon_{zz}^{n-1}|}{|\Delta\epsilon_{zz}^{n+1}|} < 10^{-4} \Rightarrow \text{END}$$
$$\text{ELSE} \quad \Rightarrow \text{plasticity algorithm} \Rightarrow \sigma_{zz}^{n} \quad \text{GOTO 3.}$$

2.8 Implementation

The present model has been implemented as a user-defined material into LS-DYNA. Starting from the additive decomposition of the strain increment at time t_{n+1}: $\Delta\boldsymbol{\varepsilon}_{n+1} = \boldsymbol{\varepsilon}_{n+1} - \boldsymbol{\varepsilon}_{n}$, the trial stress, assuming elastic behaviour, is computed as $\boldsymbol{\sigma}_{n+1}^{\text{trial}} = \boldsymbol{\sigma}_{n} + \mathbb{C} : \Delta\boldsymbol{\varepsilon}_{n+1}$. Checking the yield surface $f = f(\boldsymbol{\sigma}_{n+1}^{\text{trial}}, \bar{\varepsilon}^{pl})$ indicates elastic ($f \leq 0$) or plastic loading ($f > 0$). In the case of plastic loading a classical elastic predictor plastic corrector scheme is applied for stress integration. Here the plastic strain increment can be written as

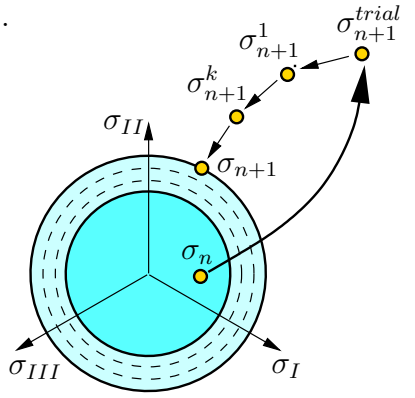

Figure 9: Cutting plane algorithm

$\Delta\bar{\boldsymbol{\varepsilon}}^{pl}_{n+1} = \bar{\boldsymbol{\varepsilon}}^{pl}_{n+1} - \bar{\boldsymbol{\varepsilon}}^{pl}_{n} = \Delta\lambda_{n+1}\boldsymbol{m}_{n+1}$ where $\Delta\lambda$ represents the sought plastic multiplier, $\boldsymbol{m}_{n+1} = \partial g(\boldsymbol{\sigma}_{n+1})/\partial\boldsymbol{\sigma}_{n+1}$ the direction of the plastic flow and g the plastic potential. The increment of the equivalent plastic strain is obtained from $\Delta\bar{\varepsilon}^{pl}_{n+1} = \Delta\lambda_{n+1}\ \|\boldsymbol{m}_{n+1}\|$. Hence, the stresses can be calculated through $\boldsymbol{\sigma}_{n+1} = \boldsymbol{\sigma}^{\text{trial}}_{n+1} - \Delta\lambda_{n+1}\mathbb{C} : \boldsymbol{m}_{n+1}$ and the internal variable is updated by $\bar{\varepsilon}^{pl}_{n+1} = \bar{\varepsilon}^{pl}_{n} + \Delta\lambda_{n+1}\ \|\boldsymbol{m}_{n+1}\|$. Inserting in the active yield surface leads formally to a nonlinear equation in $\Delta\lambda_{n+1}$ which is solved by the Newton-Raphson method.
The yield condition reads:

$$f(p, q, \bar{\varepsilon}^{pl}, \dot{\bar{\varepsilon}}^{pl}) = q - \beta(\bar{\varepsilon}^{pl}, \dot{\bar{\varepsilon}}^{pl})p - c(\bar{\varepsilon}^{pl}, \dot{\bar{\varepsilon}}^{pl}) = 0 \tag{21}$$

The plastic potential reads:

$$g = \sqrt{q^2 + \alpha p^2} \tag{22}$$

Derivation of the plastic potential g for the stress state σ gives the direction of the plastic flow:

$$\Delta\bar{\varepsilon}^{pl}_{n+1} = \Delta\lambda_{n+1}\ \|\boldsymbol{m}_{n+1}\| \quad \text{with} \quad \boldsymbol{m}_{n+1} = \partial g(\boldsymbol{\sigma}_{n+1})/\partial\boldsymbol{\sigma}_{n+1} = \frac{3}{2g}\boldsymbol{s} + \frac{\alpha p}{3}\boldsymbol{\delta} \tag{23}$$

So the update of the plastic strain tensor in rate form is:

$$\dot{\boldsymbol{\varepsilon}}^{p} = \frac{\dot{\lambda}}{g}\left(\frac{3}{2}\boldsymbol{s} + \frac{1}{3}\alpha p\boldsymbol{\delta}\right) \tag{24}$$

The stress update in rate form reads:

$$\dot{\boldsymbol{\sigma}} = 2G(\dot{\boldsymbol{\varepsilon}}_{\boldsymbol{dev}} - \dot{\boldsymbol{\varepsilon}}^{\boldsymbol{p}}_{\boldsymbol{dev}}) + K((\dot{\varepsilon}_{vol} - \dot{\varepsilon}_{vol})\boldsymbol{\delta} \tag{25}$$

$$\dot{\boldsymbol{\sigma}} = \mathbb{C}\dot{\boldsymbol{\varepsilon}} - \dot{\lambda}\frac{3G}{g}\boldsymbol{s} - \dot{\lambda}\frac{K\beta}{g}p\boldsymbol{\delta} \tag{26}$$

Applying a classical elastic predictor–plastic corrector scheme the stress update at the end of each time step reads:

$$\boldsymbol{\sigma} = \boldsymbol{\sigma}^{trial} - \Delta\lambda\frac{3G}{g^{trial}}s^{trial} - \Delta\lambda\frac{\beta K}{g^{trial}}p^{trial}\boldsymbol{\delta} \tag{27}$$

Here, the plastic multiplier $\Delta\lambda$ must be determined by a Newton iteration. The yield condition must be fulfilled at the end of the time step t_{n+1}:

$$\begin{aligned} f^{k}_{n+1} &= q^{trial} + \beta^{k}_{n+1}(\bar{\varepsilon}^{pl}, \dot{\bar{\varepsilon}}^{pl})p^{trial} - \Delta\lambda^{k}3Gq^{trial} \\ &\quad -\Delta\lambda^{k}\frac{\alpha K\beta^{k}_{n+1}(\bar{\varepsilon}^{pl}, \dot{\bar{\varepsilon}}^{pl})}{g^{trial}}p^{trial} - c^{k}_{n+1}(\bar{\varepsilon}^{pl}\dot{\bar{\varepsilon}}^{pl}) = 0 \end{aligned} \tag{28}$$

For the Newton iteration linearization around the current stress state at each iteration step k is needed. Therefore tangents with respect to $\Delta\lambda$ and $\dot{\Delta}\lambda$ for the yield surface

coefficients are required. q_{n+1}, p_{n+1} and the yield surface coefficients at time t_{n+1} are:

$$\begin{aligned} q_{n+1}^k &= q_{n+1}^{trial}\Big(1-\Delta\lambda^k\frac{3G}{g^{trial}}\Big) \\ p_{n+1}^k &= p^{trial}\Big(1-\Delta\lambda^k\frac{K\alpha}{g^{trial}}\Big) \\ \beta_{n+1}^k(\bar{\varepsilon}^{pl},\dot{\bar{\varepsilon}}^{pl}) &= \beta_n(\bar{\varepsilon}^{pl},\dot{\bar{\varepsilon}}^{pl})+\frac{\partial\beta(\bar{\varepsilon}^{pl},\dot{\bar{\varepsilon}}^{pl})}{\partial\Delta\lambda}\Delta\lambda^k+\frac{\partial\beta(\bar{\varepsilon}^{pl},\dot{\bar{\varepsilon}}^{pl})}{\partial\dot{\Delta\lambda}}\frac{\Delta\lambda^k}{\Delta t} \\ c_{n+1}^k(\bar{\varepsilon}^{pl},\dot{\bar{\varepsilon}}^{pl}) &= c_n(\bar{\varepsilon}^{pl},\dot{\bar{\varepsilon}}^{pl})+\frac{\partial c(\bar{\varepsilon}^{pl},\dot{\bar{\varepsilon}}^{pl})}{\partial\Delta\lambda}\Delta\lambda^k+\frac{\partial c(\bar{\varepsilon}^{pl},\dot{\bar{\varepsilon}}^{pl})}{\partial\dot{\Delta\lambda}}\frac{\Delta\lambda^k}{\Delta t} \end{aligned} \tag{29}$$

Inserting linearizations (29) in the yield condition (29) at the end of the time step t_{n+1} and derivation for $\Delta\lambda$ delivers the required linearization around the current stress state:

$$\begin{aligned} \frac{\partial f_{n+1}(\Delta\lambda)}{\partial\Delta\lambda} &= \Big(\frac{\partial\beta(\bar{\varepsilon}^{pl},\dot{\bar{\varepsilon}}^{pl})}{\partial\Delta\lambda}+\frac{\partial\beta(\bar{\varepsilon}^{pl},\dot{\bar{\varepsilon}}^{pl})}{\partial\dot{\Delta\lambda}}\Big)p^{trial}-\frac{3G}{g^{trial}}q^{trial} \\ &\quad -\frac{\alpha K\beta(\bar{\varepsilon}^{pl},\dot{\bar{\varepsilon}}^{pl})}{g^{trial}}p^{trial}-\frac{\partial c}{\partial\Delta\lambda}-\frac{\partial c}{\partial\dot{\Delta\lambda}}\frac{1}{\Delta t} \end{aligned} \tag{30}$$

Iteration is done, until the consistency condition is fulfilled:

$$f_{n+1}^{k+1}=f_{n+1}^k+\frac{\partial f}{\partial\Delta\lambda}d(\Delta\lambda)^k=0 \tag{31}$$

If the consistency condition at the next time step can't be fulfilled the increment $\Delta\lambda$ is improved and a next iteration step is done:

$$\Delta\lambda^{k+1}=\Delta\lambda^k+d(\Delta\lambda)^k=\Delta\lambda^k-\frac{f_{n+1}^k}{\frac{\partial f}{\partial\Delta\lambda}} \tag{32}$$

3 Results: Yield surfaces of different thermoplastics

As an example, the application of the present model due to prediction of yield for different thermoplastics is shown. The results are published in the thesis of Vogler [13]. For a review of methods commonly used in crash simulation, see [4], [3], [2] and the thesis of Koesters [12]. The results obtained by PLYS are compared to the vonMises yield criterion. It must be emphasized that this criterion is usually used in crash simulation for modelling of thermoplastics. For a better understanding, the curves given in Figure 14 to Figure 16 are plotted in both the plane stress plane and the invariant plane, also known as p-q-plane or Burzynski-plane. The following experimental results are taken from Bardenheier [14]. In the Figures 10, an acrylonitrile butadiene styrene (ABS) shows noticeable agreement. In the yield surface, this results in a softening behaviour under biaxial tension. So test data from a biaxial tensile test are regarded in addition to experimentally measured hardening curves for uniaxial compression and tension and shear tests. With PLYS the experimentally obtained yield locus can be approximated very well, whereas the Drucker-Prager model is not able to fit the experimentally obtained data adequately. As can be

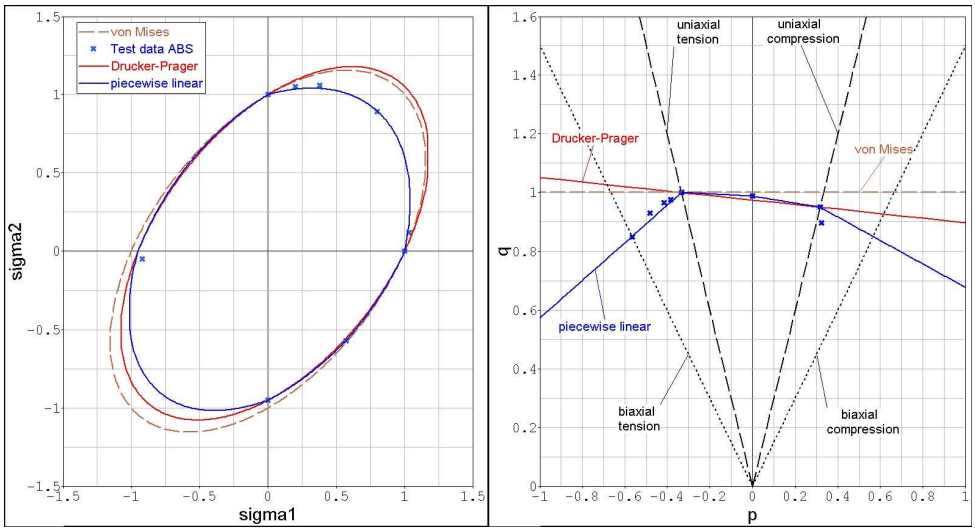

Figure 10: Yield surface of acrylonitrile butadiene styrene (ABS)

seen, using compression, tension and shear only, the yield behaviour cannot be described sufficiently. If biaxial tension is considered additionally, the yield surface is much closer to the experimental data. As a next example for a polymer that is widely used in engineering practice, polystyrene (PS) is regarded. For this polymeric material, more experimental results under different loading directions are available, see Figures 10 and 11. Again, the vonMises criterion cannot describe the challenging material response. The results obtained by PLYS are in good agreement with the experimental findings. This identifies the present model as an appropriate material law for polymers. Similar results can be observed for a polycarbonate (PC). Experimental data of biaxial tension and compression tests as well as test data of tension, compression and shear loading can be considered

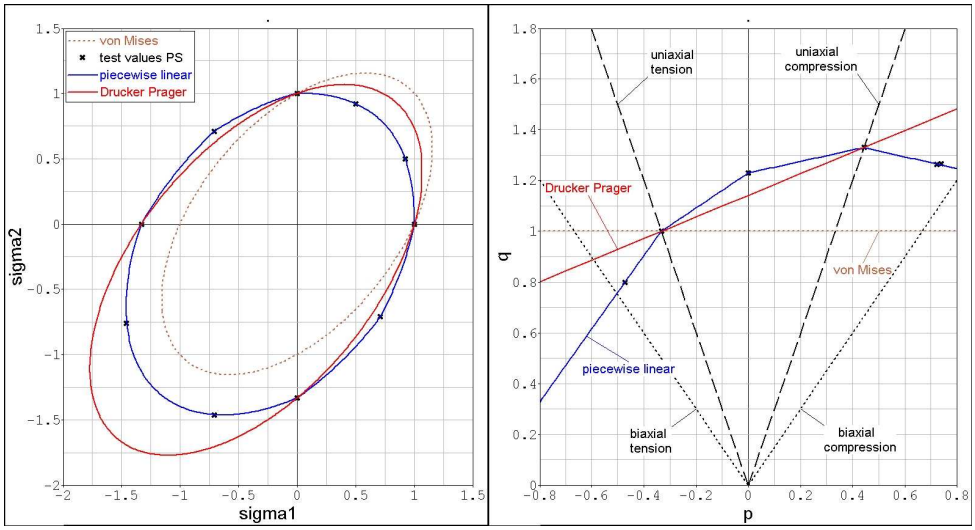

Figure 11: Yield surface of polysterene (PS)

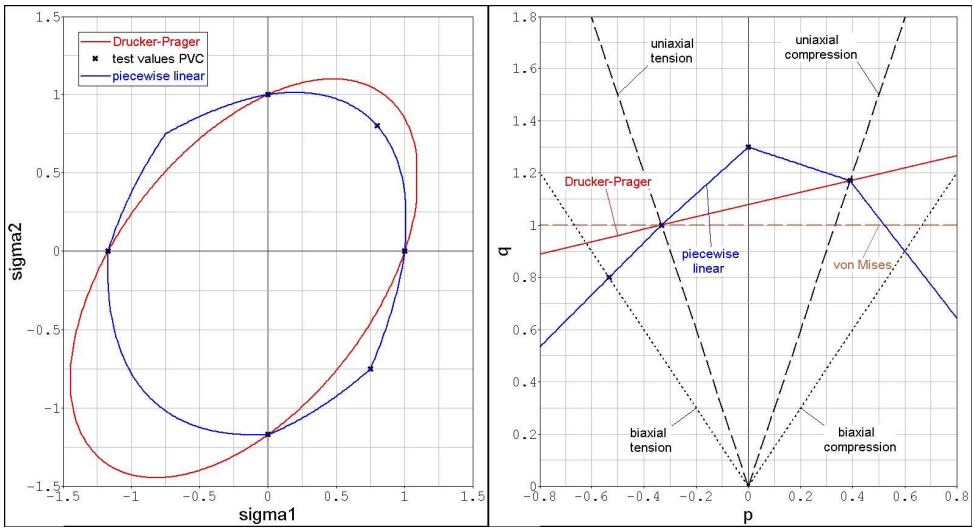

Figure 12: Yield surface of polyvinyl chloride (PVC)

simultaneously in the material model PLYS.

To sum up, the presented formulation gives a practical yet efficent approximation for typical yield surfaces of thermoplastics. As for the validation and verification procedure, the material law is one-to-one comparable to the SAMP-formulation [17]. In particular, the model is capable to fit experimental results obtained by tensile, compression, shear and biaxial tests. Furthermore, unloading and failure (realized by the presented damage and fade-out-procedure) is available as well as strain-rate dependence and non-isochoric plasticity.

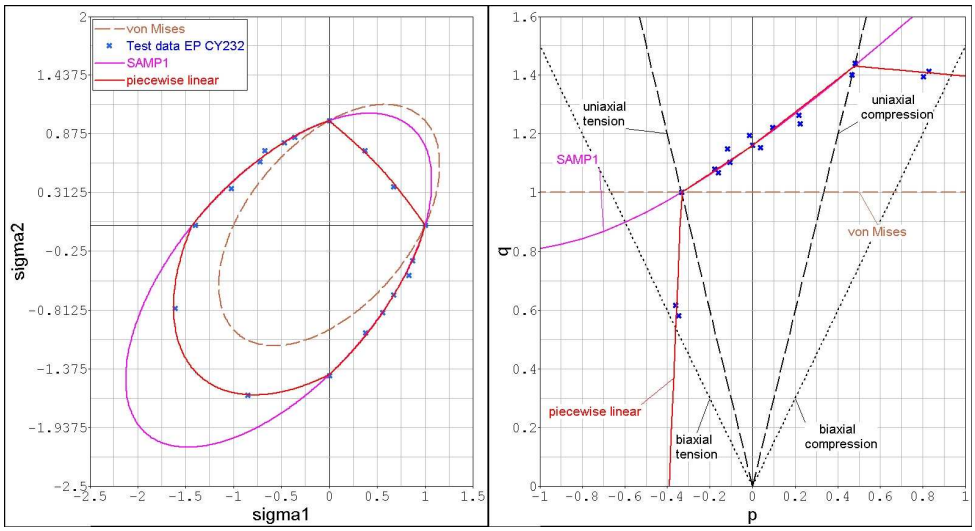

Figure 13: Yield surface of EP-resin CY232

References

[1] P.A. Du Bois, Crashworthiness Engineering Course Notes, Livermore Software Technology Corporation (2004).

[2] P.A. Du Bois, S. Kolling, M. Koesters and Frank: Crashworthiness analysis of structures made from polymers. *Proceedings of the 3rd LS-DYNA Forum, Bamberg, Germany,* ISBN 3-9809901-0-9, C-I:1–12, 2004.

[3] P.A. Du Bois, S. Kolling, M. Koesters and T. Frank: Material behaviour of polymers under impact loading. *International Journal of Impact Engineering*, 32(5):725–740, 2006.

[4] P.A. Du Bois, S. Kolling, M. Koesters and T. Frank: Modelling of polymeric materials in crashworthiness analysis. *3rd International Workshop for Material and Structural Behaviour at Crash Processes - crashMAT, Freiburg, Germany, Conference Proceedings*, 2004.

[5] A. Haufe, P.A. Du Bois, S. Kolling and M. Feucht: A semi-analytical model for polymers subjected to high strain rates. *Proceedings of the 5th European LS-DYNA Users Conference, Birmingham, England*, 2b(58):1–16, 2005.

[6] S. Kolling, A. Haufe, M. Feucht and P.A. Du Bois: A semianalytical model for the simulation of polymers. *Proceedings of the 4th LS-DYNA Forum, Bamberg, Germany,* ISBN 3-86010-795-X, A-II:27–52, 2005.

[7] M. Vogler: Implementierung von visko-plastischen Stoffgesetzen für Thermoplaste, Diplomarbeit DaimlerChrysler & BTU Cottbus (2005).

[8] M. Vogler, S. Kolling and A. Haufe: A constitutive model for polymers with a piecewise linear yield surface. *Proceedings in Applied Mathematics and Mechanics · PAMM*, 6(1):275–276, 2006.

[9] J. Lemaitre and J.-L. Chaboche: Mécanique des matériaux solides, Dunod, 1988.

[10] J.O. Hallquist: LS-DYNA, Theoretical Manual, Livermore Software Technology Corporation, Report 1018, 1991.

[11] S. Kolling and A. Haufe: A constitutive model for thermoplastic materials subjected to high strain rates. *Proceedings in Applied Mathematics and Mechanics · PAMM*, 5:303–304, 2005.

[12] M.Koesters: Materialmodellierung von Thermoplasten mit Anwendungen in der Crashsimulati-on, Diplomarbeit DaimlerChrysler & BTU Cottbus, 2004.

[13] T. Frank, A. Kurz, M. Pitzer and M. Soellner: Development and validation of numerical pedestrian impactor models. 4th European LS-DYNA Users Conference, pp. C-II-01/18, 2003.

[14] R. Bardenheier: Mechanisches Versagen von Polymerwerkstoffen. Hanser-Verlag, 1982.

[15] D.C. Drucker and W. Prager: Soil mechanics and plastic analysis or limit design. Quaterly of Applied Mathematics, 10:157-165, 1952.

[16] D.C. Drucker: A definition of stable inelastic material. Journal of Applied Mechanics, 26:101-106, 1959.

[17] A. Haufe, P.A. Du Bois, S. Kolling and M. Feucht: On the development, verification and validation of a semi-analytical model for polymers subjected to dynamic loading. *Proceedings of the International Conference on Adaptive Modeling and Simulation, ADMOS, Barcelona, Spain*, 2005.

[18] M. Junginger: Charakterisierung und Modellierung unverstärkter thermoplastischer Kunststoffe zur numerischen Simulation von Crashvorgängen", Dissertation, Fraunhofer Gesellschaft, Germany, ISBN 3-8167-6339-1.

[19] J.C. Simo and T.J.-R. Hughes: Elastoplasticity and viscoplasticity - computational aspects. Springer Series in Applied Mathematics, Springer, Berlin, 1989.

[20] T.J.-R. Hughes: Numerical implementation of constitutive models: rate-independent deviatoric plasticity. In Nemat-Nasser et al: Theoretical foundation for large scale computations for nonlinear material behaviour. Martinus Nijhoff Publishers, Dordrecht, 1984.

[21] T.J.-R. Hughes: Efficient and simple algorithms for the integration of general classes of inelastic constitutive equations including damage and rate effects. In T.J.-R. Hughes ,T. Belytschko: nonlinear finite element analysis course notes, 2003.

[22] P. Wriggers: Nichtlineare Finite-Element-Methoden, Springer-Verlag, 2001.

[23] W.W. Feng and W.H. Yang: general and specific quadratic yield functions, composites technology review.

[24] V. Kolupaev, M. Moneke and N. Darsow: Modelling of the three-dimensional creep behaviour of non-reinforced thermoplastics, Computational Materials Science 32 (3-4) (2005), 400-406.

[25] V.A. Kolupaev, S. Kolling, A. Bolchoun and M. Moneke: A limit surface formulations for plastically compressible polymers. *Mechanics of Composite Materials*, 43(3):1–18, 2007.

[26] T. Gerster, F. Huberth and M. Neumann: Dynamische Charakterisierung und Modellierung von vier Polymer-werkstoffen. Ernst-Mach-Institut für Kurzzeitdynamik, Bericht I-09/04, Freiburg/Germany, 2004.

[27] F. Huberth, S. Hiermaier and M. Neumann: Material Models for Polymers under Crash Loads - Existing LS-DYNA Models and Perspective *Proceedings of the 4th LS-DYNA Forum, Bamberg, Germany,* ISBN 3-9809901-1-7, H-I-1-12, 2005.

[28] M. Feucht and W. Fassnacht: Simulation der duktilen Rissbildung in Crashberechnungen mit Hilfe des Gurson-Modells, 17. CADFEM User's meeting, Sonthofen/Germany, 1999.

